

# The Improved Success Rate of Integer Ambiguity Resolution by Using Many Visible GPS/GNSS Satellites

\* Kentaro Kondo

Fujitsu Limited

## Abstract

This study investigates the improvement in the theoretical success rate of the integer ambiguity resolution in GPS/GNSS carrier-phase positioning by using many visible satellites. It estimates the dependence of the rate on the baseline length in relative positioning under the condition of the use of double/triple-frequency navigation signals.

The calculation results show that the use of 14 navigation satellites (i.e., seven GPS and seven Galileo ones) remarkably improves the success rate under the condition of very short baseline length, compared with the use of seven GPS ones.

The numerical reliability of the calculated success rates is strictly tested by examining the tightness of the union and minimum-distance bounds to the rate. These bounds are also shown to be effective to investigate the realization of the high success rates.

**Keywords:** GPS, GNSS, Galileo, integer ambiguity resolution, success rate, ionospheric delay, baseline length, sphere decoding.

## 1. Introduction

Correct resolution of integer ambiguities is indispensable for precise carrier-phase relative positioning with the Global Positioning System (GPS) and the global navigation satellite system (GNSS). This means that one needs an extremely high success rate and an extremely low error rate of the resolution, even in the heavily difficult resolution for non-permanent, or mobile, receivers used in realistic and unstable environments [1].

Various conditions which are intended to improve the performance of the integer ambiguity resolution have been discussed in several studies. Such conditions include the short baseline length of relative positioning [2], the use of a reference receiver network [3], the use of multiple carrier-phase measurements, or carrier frequencies [4], more visible satellites, including planned European Galileo navigation ones [5] (see Table 1). Most of these investigations, however, do not seem to touch upon the rigorous argument on the performance of the integer ambiguity resolution, which should be based on exact statistical and mathematical discussions.

This study investigates the dependence of the theoretical success rate of the fast and reliable integer ambiguity resolution in GPS/GNSS double/triple-frequency carrier-phase relative positioning on its baseline length. It estimates the success rate under the condition using up to 14 navigation satellites (i.e., seven GPS and seven Galileo ones). This study uses the accurate method in order to calculate the theoretical success rate. Single-differentiated ionospheric delay is regarded as an error under the conditions of nonvanishing baseline length with regard to the reference and rover receivers.

## 2. Equations of GPS/GNSS measurements

Let  $\rho_{q,i}^k$  and  $\phi_{q,i}^k$  denote single-differentiated GPS/GNSS code-pseudorange and carrier-phase measurements, respectively, where  $q$ ,  $i$ , and  $k$  indicate the kind of signals, the epoch of measurements, and the distinction of the satellites, respectively.

They satisfy the following equations:

$$\begin{aligned}\rho_{q,i}^k &= \mathbf{e}_i^k \cdot \mathbf{r}_i + \left(\frac{\lambda_q}{\lambda_{L1}}\right)^2 I_i^k + c\tau_{\rho,q,i} + \delta\rho_{q,i}^k, \\ \phi_{q,i}^k &= N_q^k + \psi_i^k \\ &\quad + \frac{1}{\lambda_q} \mathbf{e}_i^k \cdot \mathbf{r}_i - \frac{1}{\lambda_q} \left(\frac{\lambda_q}{\lambda_{L1}}\right)^2 I_i^k + \frac{c}{\lambda_q} \tau_{\phi,q,i} + \delta\phi_{q,i}^k.\end{aligned}$$

where  $\mathbf{r}_i$  denotes the coordinates of a receiver,  $I_i^k$  the ionospheric delay,  $\tau_{\rho,q,i}$  and  $\tau_{\phi,q,i}$  the receiver's code-pseudorange and carrier-phase clock offsets (with dependence on the kind of measurements),  $\delta\rho_{q,i}^k$  and  $\delta\phi_{q,i}^k$  the code-pseudorange and carrier-phase measurement errors,  $N_q^k$  the integer ambiguity, and  $\psi_i^k$  the wind-up phase.  $\phi_{q,i}^k$  and  $\psi_i^k$  are expressed in a unit of cycles.  $\lambda_q (= c/f_q)$  denotes the wavelength of the carrier wave (and  $f_q$  is the frequency).  $\mathbf{e}_i^k$  denotes the unit line-of-sight vector from the satellite  $k$  to the receiver, which is assumed to have been determined with sufficient accuracy.  $I_i^k$  is measured as the delay length at the frequency of GPS-L1. All measurements and error variables are assumed to have been single-differentiated, i.e., these are the variables relative to the reference receiver's ones.

The vector variable of double-differentiated integer ambiguities is denoted by  $\boldsymbol{\nu}$  in this study.

## 3. Maximum *a posteriori* success rate

A decision,  $\delta$ , maps  $\boldsymbol{\nu}$  to a value of decision parameter,  $N$

$$\delta : \boldsymbol{\nu} \xrightarrow{\text{map}} N,$$

where  $\boldsymbol{\nu}$  and  $N$  are double-differentiated float and integer ambiguities when discussing carrier-phase GPS/GNSS positioning.

Table 1: GPS and Galileo navigation satellite systems.

|                           | GPS   | Galileo  |
|---------------------------|---|--|
| operation                 | USA   | EU   |
| number of satellites      | 28  | 30   |
| orbital radius (km)       | 26,560  | 29,994   |
| year of initial operation | 1993  | (2010)   |
| signal frequencies (MHz)  | L1: 1574.42<br>L2: 1227.6<br>L5*: 1176.45<br>(* block III,<br>2012) | L1: ←<br>L5(E5a): ←<br>E5b: 1207.14<br>E6: 1278.75 |

The success rate arisen from  $\delta$  is calculated by integrating the conditional distribution of  $\boldsymbol{\nu}$  as follows:

$$\begin{aligned} \alpha_\delta &= \int_{D_\delta(\mathbf{N})} p(\boldsymbol{\nu} | \mathbf{N}) d\boldsymbol{\nu} \\ &= \sqrt{\frac{|M|}{(2\pi)^p}} \\ &\quad \times \int_{D_\delta(\mathbf{N})} \exp\left\{-\frac{1}{2}(\boldsymbol{\nu} - \mathbf{N})^T M (\boldsymbol{\nu} - \mathbf{N})\right\} d\boldsymbol{\nu}, \end{aligned} \quad (1)$$

in which  $D_\delta(\mathbf{N})$  is defined to be the acceptance region where the decision  $\delta$  chooses  $\mathbf{N}$  in the space of  $\boldsymbol{\nu}$ , and  $M$  is the inverse of the covariance matrix of  $\boldsymbol{\nu}$ . Equation (1) has used the independence of  $\alpha_\delta$  on  $\mathbf{N}$  and the assumption of the non-informativeness of  $p(\mathbf{N})$ , *a priori* distribution of  $\mathbf{N}$ .

A maximum *a posteriori* decision,  $\delta_{\text{MAP}}$ , is defined as:

$$\begin{aligned} \delta_{\text{MAP}} : \boldsymbol{\nu} &\xrightarrow{\text{map}} \mathbf{N}_{\text{MAP}}, \\ \mathbf{N}_{\text{MAP}} &= \arg \max_{\mathbf{N}} p(\mathbf{N} | \boldsymbol{\nu}). \end{aligned} \quad (2)$$

The decision is well known to maximize  $\alpha_\delta$ . Let  $\alpha_{\text{MAP}}$  denote its optimal rate and  $D_{\text{MAP}}(\mathbf{N})$  its acceptance region.

#### 4. Voronoi polytope

$D_{\text{MAP}}(\mathbf{N})$  is shaped into a congruent point-symmetrical *Voronoi polytope* in the space of  $\boldsymbol{\nu}$ , as shown in Fig. 1. Each lattice point,  $\mathbf{N}$ , resides at the center of the polytope.

*Voronoi-relevant*, i.e., adjacent, lattice points are defined, as their distinct Voronoi polytopes share facets. The adjacent lattice points can be represented as displacement vectors from a certain lattice point to its adjacent ones. Let us represent the set of adjacent integer lattice points as

$$\{\mathbf{n}_1, \mathbf{n}_2, \dots, \mathbf{n}_i, \dots, \mathbf{n}_q\}, \quad (3)$$

which contains  $q$  lattice points. This set contains all possible lattice points, but any two of them,  $\mathbf{n}_i$  and  $\mathbf{n}_j$ , should satisfy,

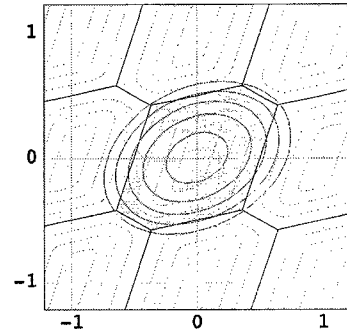


Fig. 1. Example of multivariate Gaussian distribution and the integration region for optimal success rate (Voronoi polytope).

$$\begin{aligned} |\mathbf{n}_i^T M \mathbf{n}_j| &< a_i^2, \\ a_i &= \sqrt{\mathbf{n}_i^T M \mathbf{n}_i}, \end{aligned} \quad (4)$$

in which the generalized distance,  $a_i$ , of each adjacent lattice point from the origin is introduced. The representation of (3) will not be assumed to distinguish between point-symmetrical lattice points, i.e.,  $\mathbf{n}_i$  and  $-\mathbf{n}_i$ ; thus, they are counted as one lattice point in (3).

#### 5. Methods to calculate the optimal success rate

This study calculated  $\alpha_{\text{MAP}}$  and the several upper and lower bounds by using the following algorithms on multidimensional lattices.

The LLL lattice basis reduction [6], which has polynomial-time numerical complexity, yields the approximate shortest vector of a lattice and an approximate closest vector solution (i.e., a Babai nearest plane one [7]). The former produces an upper bound,  $\alpha_{\text{B},1}$ , to the optimal success rate and the latter a lower one,  $\alpha_{\text{B}}$ , accompanied by a parallelepiped-shaped suboptimal acceptance region [8], as follows:

$$\alpha_{\text{B},1} > \alpha_{\text{MAP}} \geq \alpha_{\text{B}}, \quad (5)$$

$$\begin{aligned} \alpha_{\text{B}} &= \prod_{i=1}^p \alpha_{\text{B},i}, \\ \alpha_{\text{B},i} &= \frac{2l_{ii}}{\sqrt{2\pi}} \int_0^{\frac{1}{2}} \exp\left(-\frac{1}{2}l_{ii}^2 x^2\right) dx, \\ M &= LL^T, \end{aligned}$$

where  $l_{ii}$ 's are the diagonal elements of the lower triangular matrix,  $L$ , derived by the Cholesky factorization of  $M$ .  $M$  is assumed to have been LLL-reduced.

The improved Fincke-Pohst algorithm [9], or *sphere decoding*, which is bootstrapped by a Babai nearest plane solution and has exponential-time numerical complexity, yields the shortest (i.e., minimum-distance) vector of a lattice, the closest vector solution, and the set of Voronoi-relevant lattice points. The first also produces an upper bound,  $\alpha_{\text{MAP,MD}}$ , to  $\alpha_{\text{MAP}}$  and the third a lower one,  $\alpha_{\text{MAP,UB}}$ , as follows:

$$\alpha_{\text{MAP,MD}} > \alpha_{\text{MAP}} > \alpha_{\text{MAP,UB}}, \quad (6)$$

$$\alpha_{\text{MAP,MD}} = \min_i \alpha_{\text{MAP},i},$$

$$\alpha_{\text{MAP,UB}} = 1 - \sum_{i=1}^q \beta_{\text{MAP},i},$$

$$\begin{aligned} \alpha_{\text{MAP},i} &= 1 - \beta_{\text{MAP},i} \\ &= \frac{2a_i}{\sqrt{2\pi}} \int_0^{1/2} \exp\left(-\frac{1}{2}a_i^2 x^2\right) dx, \end{aligned}$$

where the generalized distances,  $a_i$ 's, in (4) are used.  $\alpha_{\text{MAP,UB}}$  is a well-known union bound.

The above-mentioned closest vector solution derived from sphere decoding produces the optimal success rate through executing a Monte-Carlo integration [10].

The bounds,  $\alpha_{\text{MAP,MD}}$  and  $\alpha_{\text{MAP,UB}}$ , tend to be tight under the conditions of the high success rate of ambiguity resolutions. The simultaneous tightness of upper and lower bounds discharges us from executing Monte-Carlo integrations, which require huge amount of computations especially under such conditions.

## 6. Calculation results

This study calculated the dependence of the optimal success rates,  $\alpha_{\text{MAP}}$ 's, of integer ambiguity resolution on *a priori* standard deviation in single-differentiated ionospheric delay,  $\sigma_{\Delta I}$ .

$\alpha_{\text{MAP}}$ 's were calculated chiefly by using Monte-Carlo integrations [10]. The calculation conditions are shown in Table 2. We used the assumption that  $\sigma_{\Delta I} = \Delta L \times 10^{-6}$  [11]. The constellation of satellites is shown in Fig. 2. The double- and triple-frequency conditions were examined by this study. The Galileo L1 and E5b signals were chosen for the former and the L1, E5b, and E6 ones for the latter.

The calculation result indicates that  $\alpha_{\text{MAP}} > 0.999999$  under the condition of 14 visible satellites and the 13 km or shorter baseline length as shown in Fig. 3. The condition of many satellites remarkably improves the success rates as compared with that of seven satellites (i.e., GPS ones only).

Furthermore, the use of triple-frequency signals and 14 satellites is shown to improve the success rate under the condition of the 7 km or shorter baseline length as compared with that of double-frequency signals.

This study also examined the tightness of the nearest-plane bounds,  $\alpha_{\text{B},1}$  and  $\alpha_{\text{B}}$  in (5), and the sphere-decoding ones,  $\alpha_{\text{MAP,MD}}$  and  $\alpha_{\text{MAP,UB}}$  in (6), as shown in Fig. 4. Figs. 4(a) and 4(b) investigate the condition of 14 visible satellites and triple-frequency signals. The result indicates that  $\alpha_{\text{MAP,UB}}$  and  $\alpha_{\text{MAP,MD}}$  are extremely tight under the condition of  $\alpha_{\text{MAP}} > 0.99$  and  $\alpha_{\text{MAP}} > 0.999999$ , respectively. Both of the nearest-plane bounds are, however, loose or unstable as shown in Fig. 4(a).

The bounds under the condition of seven satellites represent similar tightness to those under the condition of 14 satellites as shown in Fig. 4(c). The different behaviors are, however, discerned in the sphere-decoding bounds as follows:  $\alpha_{\text{MAP,UB}}$  tends to be loose under the condition of  $\alpha_{\text{MAP}} < 0.9$ . The untightness of  $\alpha_{\text{MAP,MD}}$  appearing at  $\sigma_{\Delta I} \sim 5$  mm is caused by the accidental degeneracy of short lattice vectors.

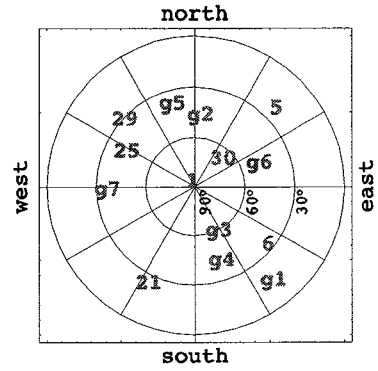


Fig. 2. Constellation of GPS (denoted by their PRN numbers) and Galileo (denoted by **gn**) satellites.

Table 2: Parameters for calculations.

|  |                     |
|--|---------------------|
| number of GPS satellites   | 7                   |
| number of Galileo satellites   | 7                   |
| standard deviation in the error in single-differentiated carrier phase measurements    |                     |
| • time-varying component   | 0.02 cycle          |
| • time-constant component  | 0.02 cycle          |
| standard deviation in the error in single-differentiated code pseudorange measurements |                     |
| • time-varying component   | 0.5 m               |
| • time-constant component  | 0.5 m               |
| AR(1) coefficient in time-varying component  |                     |
| • carrier phase measurements   | 0.95                |
| • code pseudorange measurements  | 0.5                 |
| measurement rate   | 1 epoch/sec         |
| measurement time   | 1 sec               |
| <i>a priori</i> standard deviation in single-differentiated ionospheric delay          | $\sigma_{\Delta I}$ |

## 7. Conclusion

This study theoretically investigated the improvement in the success rate of the integer ambiguity resolution by using many visible navigation satellites and estimated its dependence on the baseline length in relative positioning.

The remarkable improvement in the rate was confirmed by using 14 satellites especially under the condition of very short baseline length, compared with the use of seven GPS ones.

The numerical reliability of the calculated success rates was rigorously examined by testing the tightness of sphere-decoding bounds, i.e., union one and minimum-distance one. These tight bounds were shown to be effective to investigate the high success rate of the integer ambiguity resolution and discharge us from executing laborious Monte-Carlo integrations.

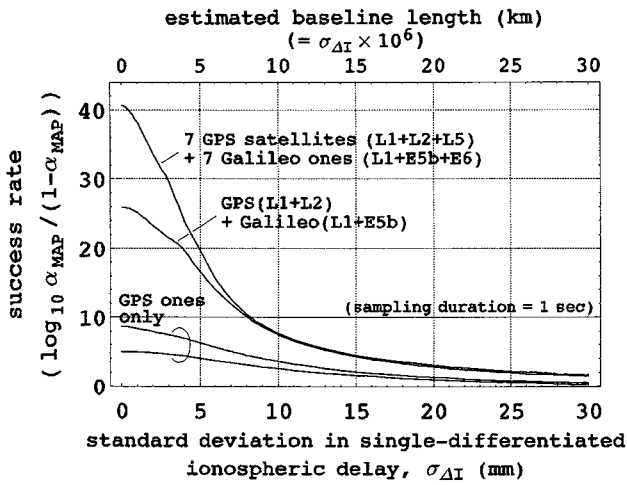
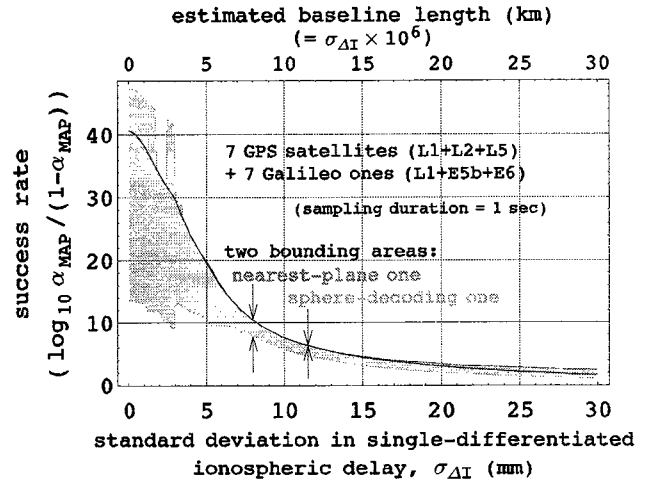


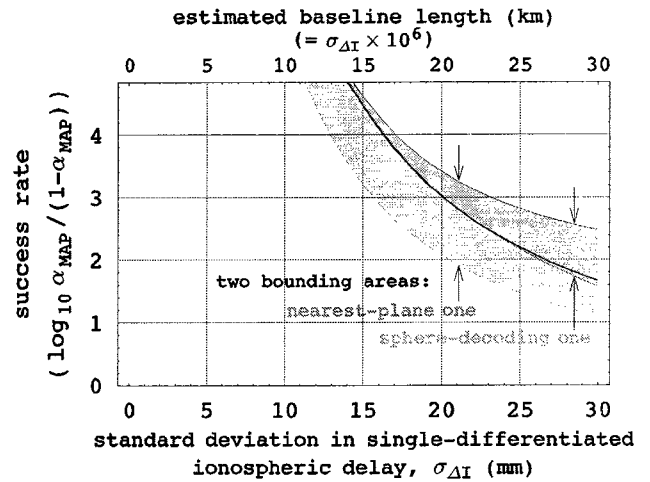
Fig. 3. Calculated success rates.

### References

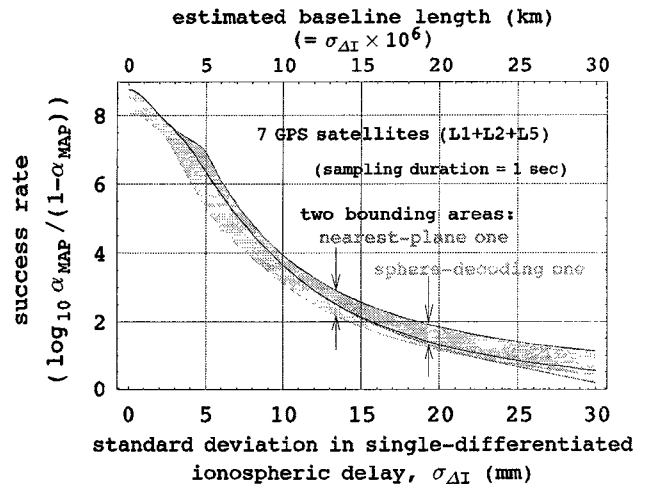
1. K. Kondo, "Centimeter-level-precise and sustentive location positioning for mobile vehicles in urban environments using multiple carrier-phase Global-Positioning-System (GPS) measurement," in *Proc. 8th World Congress on Intelligent Transport Systems*, Sydney, Australia, Sept. 30-Oct. 4, 2001, paper ITS00337.
2. M. Pratt, B. Burke, and P. Misra, "Single-epoch integer ambiguity resolution with GPS L1-L2 carrier phase measurements," in *Proc. ION GPS-97 Conference*, Kansas City, MO, Sept. 16-19, 1997, pp. 1737-1746.
3. L. Wanninger, "Improved ambiguity resolution by regional differential modelling of the ionosphere," in *Proc. ION GPS-95 Conference*, Palm Springs, CA, Sept. 12-15, 1995, pp. 55-62.
4. R. Hatch, "The promise of a third frequency," *GPS World*, vol. 7, no. 5, pp. 55-58, 1996.
5. G. W. Hein, J. Godet, J.-L. Issler, J.-C. Martin, R. Lucas-Rodriguez, and T. Pratt, "The Galileo frequency structure and signal design," in *Proc. ION GPS 2001 Conference*, Salt Lake City, UT, Sept. 11-14, 2001, pp. 1273-1282.
6. A. K. Lenstra, H. W. Lenstra, Jr., and L. Lovász, "Factoring polynomials with rational coefficients," *Math. Ann.*, vol. 261, no. 4, pp. 515-534, 1982.
7. L. Babai, "On Lovász' lattice reduction and the nearest lattice point problem," *Combinatorica*, vol. 6, no. 1, pp. 1-13, 1986.
8. P. J. G. Teunissen, "Success probability of integer GPS ambiguity rounding and bootstrapping," *J. Geodesy*, vol. 72, no. 10, pp. 606-612, 1998.
9. E. Agrell, T. Eriksson, A. Vardy, and K. Zeger, "Closest point search in lattices," *IEEE Trans. Inform. Theory*, vol. 48, no. 8, pp. 2201-2214, 2002.
10. K. Kondo, "The accurate optimal-success/error-rate calculations applied to the realizations of the reliable and short-period integer ambiguity resolution in carrier-phase GPS/GNSS positioning," *IEEE Trans. Inform. Theory*, submitted for publication.
11. B. Schaffrin and Y. Bock, "A unified scheme for processing GPS dual-band phase observations," *Bull. Geod.*, vol. 62, pp. 142-160, 1988.



(a) fourteen-satellite case



(b) the same case as (a), but vertically magnified



(c) seven-satellite case

Fig. 4. Examination of calculated success rates and bounds.